Chapter 10

Finite Element Analysis Applications in Failure Analysis: Case Studies

Ahmad Ivan Karayan, Deni Ferdian, Sri Harjanto,
Dwi Marta Nurjaya, Ahmad Ashari and Homero Castaneda

Additional information is available at the end of the chapter

http://dx.doi.org/10.5772/51024

1. Introduction

The use of the finite element in engineering applications has grown rapidly in recent years. Finite element analysis (FEA) is based on numerical computation that calculates all parameters and boundaries given. Supported with powerful computer processors and continuous software development, the finite element method is rapidly advancing. The use of finite element analysis is not limited to the engineering field, as there are also medical and geospatial applications. The early development of the finite element can be traced back to the work of Courant [1], followed by the work of Martin [2], which applied the solutions for structural analyses at Boeing Company in the 1950s. Further work by Argyris, Clough, Turner, and Zienkiewicz developed the governing mathematical equation for the finite element method [3].

The numerical simulation introduced in the 70s for the stress model on concrete as published by Hillerborg [4] is a clear example of the FEA concept. Huiskes *et al.* [5] also stated that the finite element has been used in a structural stress analysis of human bones for biomechanic applications. Zienkiewicz *et al.* [6] applied the finite element method to the linear and non-linear problems encountered during the analysis of a reactor vessel. Gallagher [7] studied brittle material design through use of the finite element method, which incorporated thermal and elastic analysis aspects of the overall design. Miller *et al.* [8] used the finite element method during the study of crack stability of a turbine blade and proposed a hypothesis based on material strength characteristics, plastic zone size/history, and residual plastic strains.

In the mid 80s, Oritz *et al.* [9] proposed a method that aimed to enhance the performance of general classes of elements that undergo strain localization. An overview of the application of the finite element in machining from the 70-90s was well documented by Mackerle [10].

The application of the method to localize fractures was studied by Broberg [11], and further work was continued by Borst *et al.* [12]. Nowadays, finite element analysis is widely used by the engineering field in fluid dynamic and electrical applications.

In general, the finite element analysis is widely used in the pre-production manufacturing process to determine the most cost-effective decision based on the analysis. Finite element simulations allow comparison between different "designs." Finite element analysis can simulate operational and environmental conditions and formulate modifications without creating a physical prototype.

In order to adequately determine the root cause of material failure, two outcomes are required: the answer and an explanation. The failure of a mechanical component is usually associated with materials, the environment, a third party, or human error. An investigation through metallurgical failure analysis is usually conducted to reveal the root cause and the failure mechanism. Work by Griffith [13] on fracture mechanics created a breakthrough in the understanding of the material fracture mechanism. In certain cases, a conventional failure analysis approach is not enough to reveal the failure, and therefore, a more comprehensive analysis through the finite element is needed. Prawoto *et al.* [14] explained that the use of the finite element is an effective approach when the causes of failure are determined using qualitative metallographic and fractographic testing. The finite element requires an understanding of how a component works and will support the correct information and data. The quality of the data provided is a key element for the successful outcome of the simulation.

2. The finite element in failure analysis

The use of finite element analysis in mechanical applications has heavily increased in recent years. The continuous efforts to improve calculations and analyses so that models accurately incorporate actual conditions have been rewarded as a consequence of computer tool evolution. The finite element analysis has become an important tool for improving the design quality in numerous applications. The finite element analysis is a computer-based technique to solve problems using numerical solutions. The analysis includes a method based on creating a geometrical model of the structure that is divided into individual nodes or elements.

Finite element modeling provides different insights into the engineering analysis that cannot be obtained with the classical failure analysis method. Classical commercial software such as ABAQUS® and ANSYS® has been widely used to analyze failures or defects and reconstruct possible root causes. The images and animation produced by the software help to give a better understanding by visualizing the root cause behind the failure event. Previously, the development of the finite element evolved slowly due to a lack of tools to solve mathematical equations, and therefore, the method remained dormant until the computer era.

The early finite element software was commissioned by NASA in mid 1960s, which introduced NASTRAN® as an application that helped to design more efficient structures for vehicles that were developed by them [15]. The ANSYS® software, which was released in

1970, was run on a massive mainframe computer that was less powerful than the personal computers of today [16]. The early software was only capable of simulating the 2D beam model, but it eventually progressed towards the modern 3D solid model of today as computer hardware developed.

The applications of finite element analysis in engineering failure analysis are in continuous evolution as more factors related to the failure event are taken into account. For example, in the case of turbine blades involved in jet engine failure, engineers should incorporate the thermal effect and load effect received by the blade in the simulation, not to mention other possibilities from foreign particles that could initiate the failure. Therefore, FEA calculations now incorporate a combination of multiple physical environments. Current research related to the application of the finite element in failure analysis has been published in peer-reviewed journals, and can be seen in publications such as *Engineering Failure Analysis Journal*® and *Failure Analysis and Prevention Journal*®.

In general, a finite element method consists of three phases: (1) pre-processing, where the analyst creates the finite element mesh and applies certain parameters or boundaries to the model, (2) solver/solution, where the program runs the governing mathematical equation that was created by the model, and (3) post-processing, where the result is evaluated and validated for further interpretation.

Some limitations must be recognized in the finite element method. The ability to define and analyze the system and the model will determine the quality of the simulation results. The evaluations of any failure event need a comprehensive approach to reveal the root cause of the failure. FEA is a tool where multidisciplinary fields are combined to help find or support the solution with better accuracy for a final conclusion. Below are three case studies that illustrate how finite element analysis can be utilized in failure analysis.

3. FEA in mechanical failure

The use of FEA for mechanical failure has become a necessary tool that is easily obtained, as the commercial software is readily available for users. FEA is widely used in failure analysis assessment when analyzing and characterizing the quantitative and qualitative approaches used to determine the root cause of an event leading to a failure. The software is given historical background information related to the failure along with other boundary conditions. Below is an example of a mechanical failure analysis assessment that used finite element analysis software to verify the findings regarding the failure event.

In the first case, the finite element method was used to analyze the stress distribution of a failed 28MW horizontal hydroturbine shaft [17]. The data corresponded to the fractography and metallographic observations. The finite element analysis was performed for normal conditions as well as the type of high load conditions that would be experienced during the start-up period.

The shaft was constructed by the joining of a forged and cast part by slag welding. A crack was observed at the radius area of the casted part. The part was given an estimated 200,000

hours of operating life, and failure was detected after 163,411 hours in service. A visual examination of the fracture surface showed a fatigue pattern with obvious ratchet marks. Further observation of the fracture surface showed visible distorted fatigue lines around numerous gas holes and areas of increased porosity.

An original document indicated that the shaft was heat-treated to complete an austenization process. However, metallographic examination showed cast ferrite-pearlite with an undissolved dendrite structure, which might indicate that an improper heat treatment process occurred. In addition, a large non-metallic inclusion was also observed in the cast part.

A linear FEA was used to determine the stress state of the turbine shaft and shaft flange. The commercial ANSYS® software was used for the finite element modeling. The model represents a discrete continuum by an 8-node finite element with three degree of freedom that comprises 49,430 nodes and 47,547 elements. All of the boundary conditions were incorporated into the model.

A numerical calculation to determine the shaft flange stress states was performed for two characteristic load cases, where one load was taken from the manufacturer's documentation and the second load was the static load that occurs during start-up. Calculation of the finite element for both load conditions showed that the maximum stress was at the crack initiation site at the shaft flange.

The data collected from the chemical composition test and mechanical test showed that the material did not comply with the minimum standard required. Therefore, the crack location where the failure occurred was more susceptible to stress. Finite element analysis showed a high distribution of stress at the failed area. The finite element analysis revealed that the obtained tensile stress value on the shaft flange transition radius due to the load in case 2 was higher than recommended, and was characterized by the stress intensity factor at the crack tip being higher than the material threshold.

It was concluded that corrosion fatigue was the cause of the shaft failure [16]. The root cause for this case was improper corrosion protection at the failed area and a lack of periodical inspection, both of which were necessary due to the high stress on the region.

4. FEA in corrosion failure

Karayan *et al.* [18] studied the failure of a seawater inlet pipe. The failure was first characterized by a small leak at approximately the 4-8 o'clock position. A schematic drawing of the inlet pipe showing the backing bar near the leak location is shown in Figure 1. This backing bar was installed on the welded surface. The visual examination of this failed pipe is shown in Figure 2. In order to find out the root cause of failure, a number of laboratory tests were performed. The results showed that the failure was caused by cavitation, as evident by the presence of a crater-like surface near the backing bar (Fig. 3). These localized craters seemed unusual since they were only noticed near the backing bar. An additional tool such as finite element analysis was used to determine why this was the case. A finite

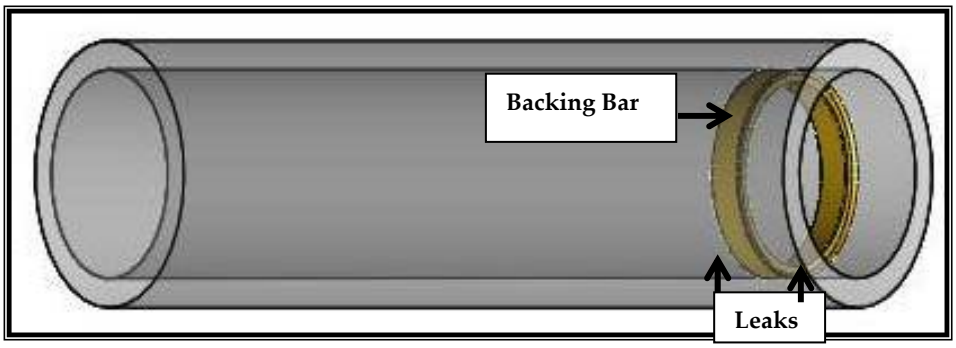

Figure 1. Big and small leak near the backing bar at about 6 o'clock position viewed from the inner side of seawater inlet pipe.

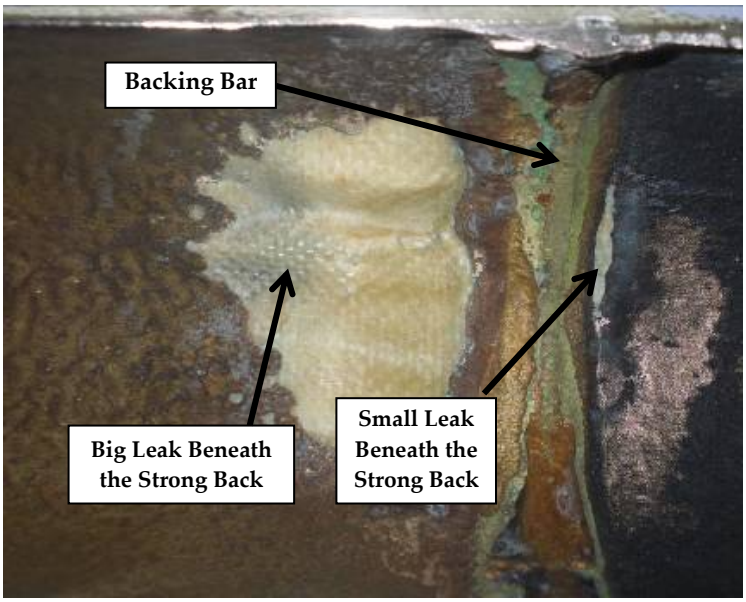

Figure 2. Big and small leak near the backing bar at about 6 o'clock position viewed from the inner side of seawater inlet pipe.

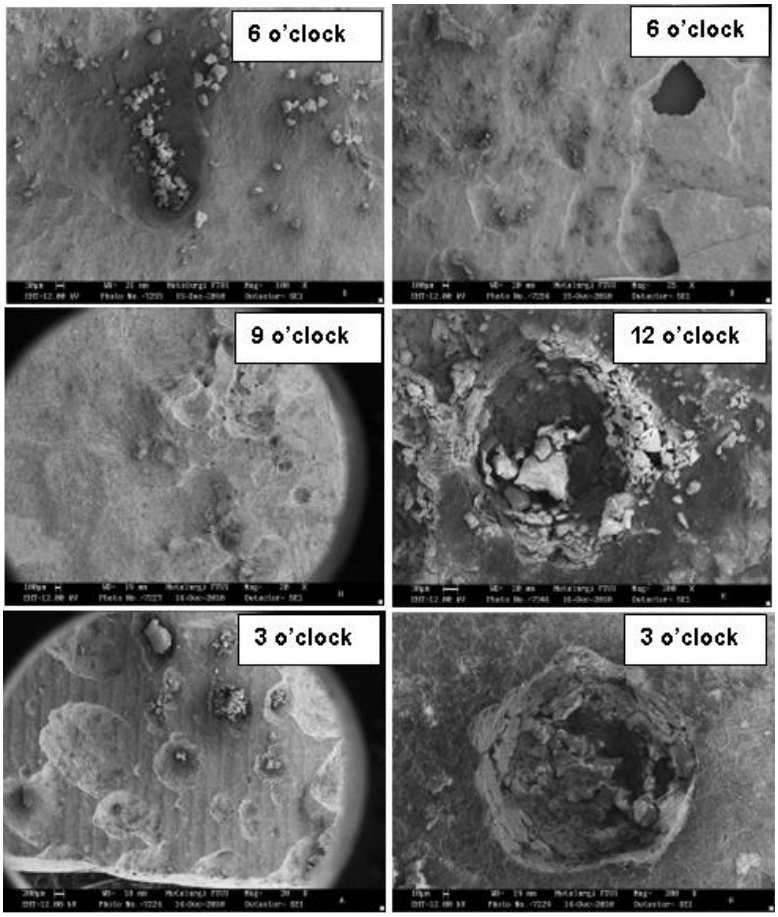

Figure 3. Surface morphologies of brown crater – like surface taken from 6 – 3 o'clock position.

element analysis was executed based on the pipe dimension and actual fluid conditions such as velocity, pressure, temperature, and implicit parameters. Because there were no data for the initial height of the unwanted backing bar, the authors assumed that the initial height was the highest backing bar found on the specimen. Interestingly, the failure location predicted by the finite element analysis matched up with the actual evidence (Fig. 4). It precisely showed that the failure could be located around the backing bar where the eddy zone was formed in this area. This suggests that sometimes the results obtained from laboratory tests cannot explain why a failure occurs, although evidence indicates the existence of a certain problem. In this case, a finite element analysis is the only tool that can help a failure analyst find the root cause of failure. As can be seen from Figure 4, the leaks and crater-like surfaces found in the area near the backing bar were attributed to the formation of eddy zones in this area. The length of the eddy zone predicted that the area that might suffer from a flow-induced attack.

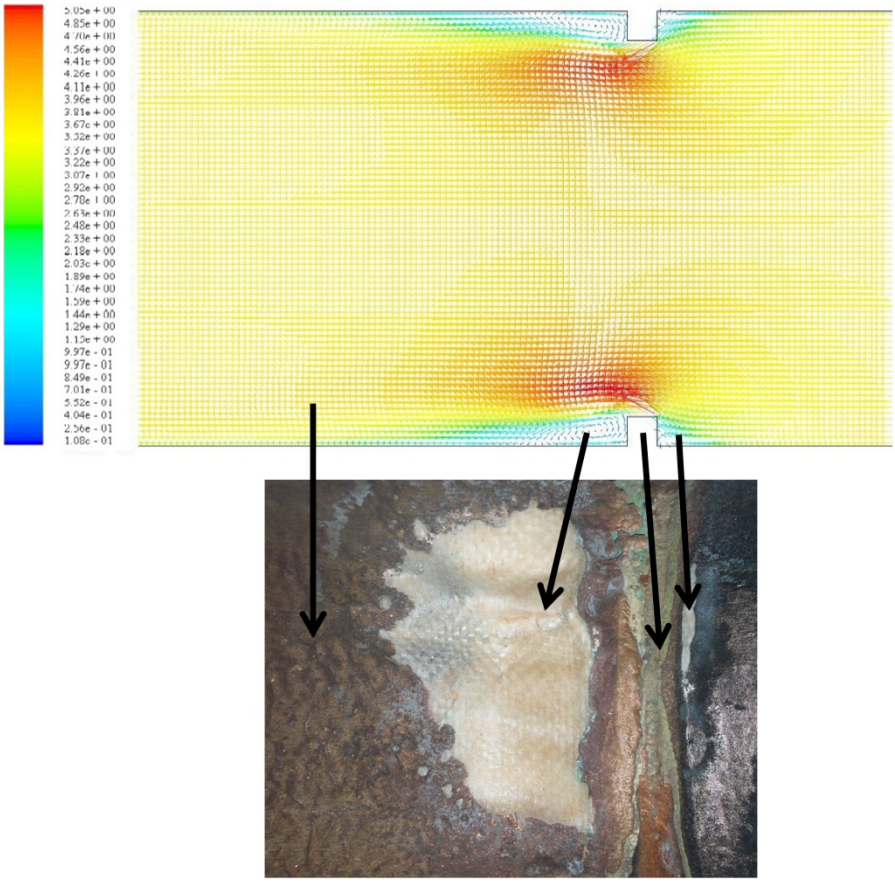

Figure 4. Finite element analysis of the inner pipe showing the orifice effect and the eddy zone near the backing bar correlated with the actual leaks on the inlet pipe.

The last case is a trunkline that burst during service [19]. This incident produced a significant impact on the gas production of the company and also on the environment. The failure was characterized by a mesa-like attack and wall thinning at the 5-7 o'clock position on the inner surface. The location of failure is shown in Figure 5. A reddish brown corrosion product was noticed on the surface, but there with no indication of the occurrence of an H_2S attack found in the material. This trunkline, carrying the gas with a total pressure of 905 psi, spanned across the jungle in the descending position. The analysis of the gas composition is listed in Table 1. The topography and characteristics of the soil in which the trunkline was located and also the material specification data is listed in Table 2.

Figure 5. The specimen sent to the laboratory for analysis is indicated by arrow

Component		Mole %
H_2	Hydrogen	0.0000
O_2	Oxygen	0.0084
N_2	Nitrogen	3.6036
CO_2	Carbon Dioxide	1.9406
H_2S	Hydrogen Sulfide	0.0000
C_1	Methane	82.7838
C_2	Ethane	6.7222
C_3	Propane	3.0077
iC_4	Iso-Butane	0.6144
nC_4	n-Butane	0.6610
iC_5	Iso-Pentane	0.2384
C_5	n-Pentane	0.1418
C_6	Hexanes	0.1352
C_7	Heptanes	0.0982
C_8	Octanes	0.0306
C_9	Nonanes	0.0072
C_{10}	Decanes	0.0069
C_{11+}	Undecanes plus	0.0000

Table 1. Result of gas analysis in trunkline

Item	Description	Result
Property	Q	± 3 MM
	WC	-
	GOR	-
	P (Psi)	750
	T (F)	140
Fluid Composition	H_2S	0.00
	CO_2 (%)	1.9406
	SRB content	-
	Chloride (%)	0.7635
	Water (%)	0.0898
Pipe Arrangement	Laydown/buried/support w/ith trestle	Laydown
	Seam position	-
Corrosion Form	Uniform/localized/pitting/etc	pitting/localized
	external/internal/both	Internal
	On seam/not	-
	On 6 o'clock/others	6 o'clock
Environment	Elevation	Descending
	Any river/road crossing	No
	Soil pH	-
	Any trees/bushes	Yes
Document	Work over on wells using the line	No job in last one year
	WT inspection	not yet

Table 2. Fluid properties and failed trunkline condition.

A visual examination showed that the burst area was located at the 6 o'clock position of the (a) downstream part and the (b) upstream part (Fig. 6). Some points on the inner surface of the downstream part at the 5-7 o'clock position showed surface degradation with wall thinning and pits (Fig. 7). Some points on the inner surface of the upstream part at the 5-7 o'clock position also showed surface degradation with wall thinning and pits (Fig. 8). A uniform attack at the burst area from the 5-7 o'clock position is shown in Figure 9.

(a)

(b)

Figure 6. (a) Downstream part and (b) upstream part showing the burst located at 6 o'clock position.

Figure 7. Wall thinning and pits at 5 – 7 o'clock position of downstream part.

Figure 8. Wall thinning and pits at 5 – 7 o'clock position of upstream part.

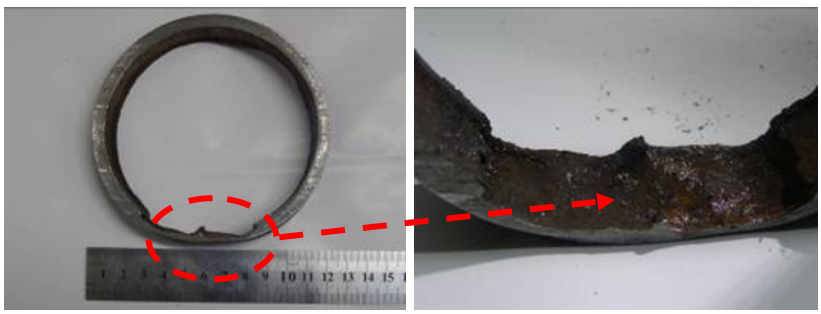

Figure 9. Uniform attack at the burst area from 5-7 o'clock position.

The metallographic preparation and macroetching were performed on the perimeter of the trunkline, and the results showed that the trunkline was made of seamless pipe (Figs. 10 and 11). The thinning area shown in Figure 9 was an ERW (electric resistance welding)-free area (Fig. 10). This information indicates that the failure could not be attributed to the ERW pipe issue.

Figure 10. Results of macroetching showing the absence of ERW.

Figure 11. Macrograph of 5-7 o'clock position showing the absence of ERW.

The microstructure of the trunkline was taken from the cross-section, and the results are displayed in Figure 12. As can be seen, the trunkline is composed of ferrite (light phase) and pearlite (dark phase) with equiaxed grains, which is typical of seamless pipe. The chemical composition of the trunkline was tested using an optical emission spectrometer and the results (Table 3) show that this trunkline is composed of an API 5L X60 steel [20]. Due to the insufficient geometry of the trunkline, the mechanical property of the trunkline was only examined by hardness testing. In order to verify that the specification of this material was API 5L, the resultant hardness values were converted to tensile strength (Table 4).

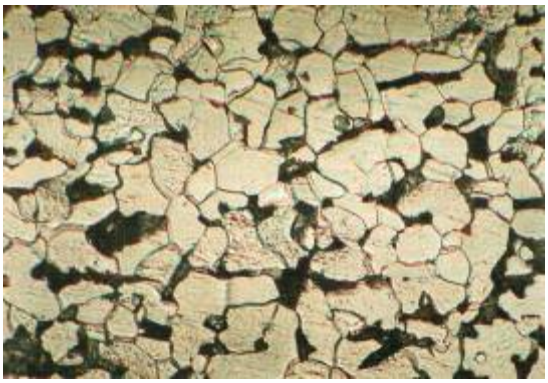

Figure 12. Microstructure of trunkline showing a typical seamless microstructure with equiaxed grains. The dark phase is pearlite and the light one is ferrite.

Material	C (%)	Mn (%)	P (%)	S (%)	Ti (%)
API 5L X60 PSL 1 [20]	0.22	1.40	0.030 (max) <	0.030 (max)	0.040
Failed Trunkline	0.165	0.594	0.003	< 0.003	< 0.002

Table 3. Chemical composition of trunkline

Material	*Average HRB*	*Approxmate UTS Based on Conversion (MPa)*
Failed trunkline	82	524
API 5L X60 [20]	-	517 (min)

Table 4. Converted tensile strength in comparison with API 5LX60 specification.

The finite element analysis was executed around the overfill, and the results (Fig. 13) showed that the area at which the pipe burst had a dead or eddy zone due to the excessive overfill (Figs. 14 and 15). Because there was no information about the initial overfill height, we assumed an overfill height of 1 cm for the finite element simulation. This selection was based on the fact that there was one point at the remaining overfill that had a height of 1 cm. The other areas were mostly degraded, with heights of less than 0.5 cm. Severe corrosion was noticed on every peak of overfill.

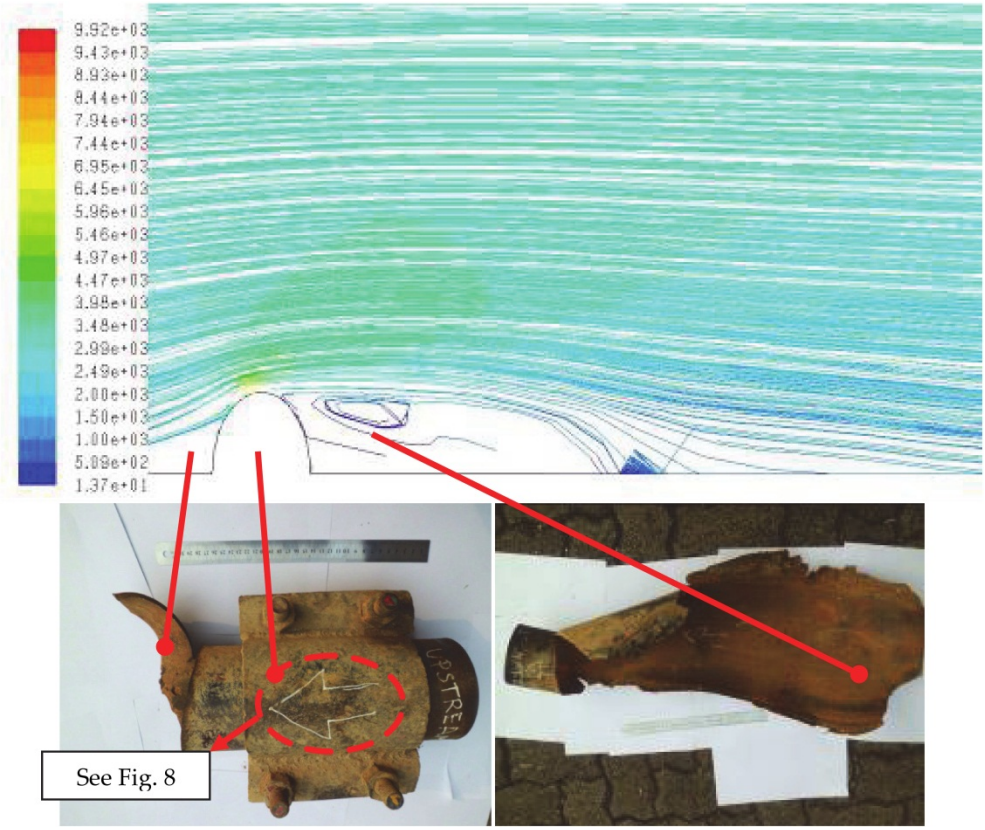

Figure 13. Finite element analysis showing the eddy zone due to overfill in comparison with the actual failed area of pipe.

As can be seen in Table 1, the only corrosive gas in the fluids flowing in this failed trunkline was CO_2. Carbon dioxide systems are one of the most common environments in the oil and gas field industry where corrosion occurs. In a relatively slow reaction, carbon dioxide forms a weak acid known as carbonic acid (H_2CO_3) in water, but the corrosion rate of CO_2 is greater than that of carbonic acid. Cathodic depolarization may occur, and other attack mechanisms may also occur. The presence of salts is relatively unimportant in sweet (CO_2) service [21], and thus, the presence of chloride in this system (0.7635%) did not significantly contribute to the failure.

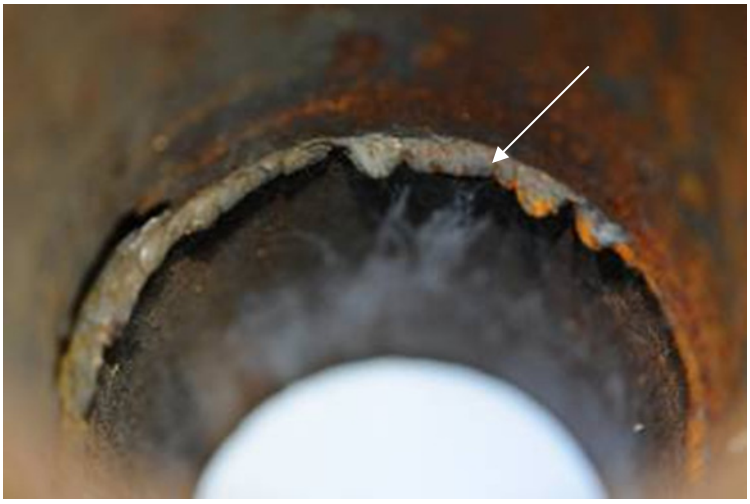

Figure 14. The inner side of circle area in Fig. 11 showing an excessive overfill (arrow) in the failed pipe at 12 o'clock position.

Figure 15. An excessive overfill and severe surface degradation beside overfill at 6 o'clock position.

The sweet environment of this system with a CO_2 partial pressure of 17.56 psig may influence the presence of corrosion. The relationship between corrosion tendency and CO_2 partial pressure in the sweet environment with pH 7 or less has been reported elsewhere [22]. When the CO_2 partial pressure is less than 7 psig, the system is non-corrosive. When it

is somewhere between 7-30 psig, corrosion in the system may be present. Lastly, when it is higher than 30 psig, the system is corrosive [22]. Temperature and flow regime are closely linked because CO_2 corrosion is dynamic and very sensitive to electrochemical and physical imbalances (especially fluctuating pressure, temperature, and volume). Steady-state (P,T,V,) conditions tend to promote protective film compaction, and therefore, passivation and low corrosion rates. Lower temperatures <120°F (approximately 50°C) tend to promote patchy corrosion with softer multi-layered iron carbonate (siderite) scales that provide some barrier protection up to 140-160°F (60-70°C). Above these temperatures, damaging localized corrosion is observed as films lose stability and spall off, giving rise to galvanic mesa attack [23]. The failed pipe we studied with an operating temperature of 140°F might have formed a protective film. However, the phenomenon of film removal and its effect on the failure of this trunkline was not evident in our laboratory test. Our finite element analysis in the failed area in Figure 13 shows the unstable and chaotic flow in the failed area (called the dead or eddy zone). As illustrated, the eddy zone was triggered by the excessive overfill. This suggests that the pipe surface in this eddy area was severely attacked by flow. The presence of a passive carbonate layer could not protect the surface from this type of flow-induced attack that led to a mesa attack.

5. Conclusions

The three case studies discussed in this chapter have clearly shown us that finite element analysis (FEA) is an excellent and powerful tool that can be employed in failure analysis. Finite element analysis provides a failure analyst with more quantitative and qualitative information about the causes of failure. Although visual examinations and laboratory tests may not be able to determine a failure mechanism, the results of finite element analysis will support all data obtained from these tests. As long as a competent analyst running the finite element analysis is given sufficient data and has good knowledge of the system under study, the results of FEA will be reliable, although they should always be validated with experimental or real condition information.

Author details

Ahmad Ivan Karayan and Homero Castaneda
Department of Chemical and Biomolecular Engineering, The University of Akron, USA

Deni Ferdian, Sri Harjanto, Dwi Marta Nurjaya and Ahmad Ashari
Department of Metallurgy and Materials Engineering, University of Indonesia, Indonesia

Deni Ferdian, Sri Harjanto, Dwi Marta Nurjaya and Ahmad Ashari
Center for Materials Processing and Failure Analysis (CMPFA), University of Indonesia, Indonesia

6. References

[1] F. Williamson, *Richard Courant and the finite element method: A further look,* Historia Mathematica, Vol 7(4), 1980, pp. 369-378.

[2] H. C. Martin, Large Deflection and Stability Analysis by Direct Stiffness Method, JPL Technical Report No. 32-931, California Institute of Technology, August 1966.
[3] R. W. Clough, Early History Of The Finite Element Method From The View Point of a Pioneer, International Journal For Numerical Methods In Engineering, 60, 2004, pp. 283–287.
[4] A. Hillerborg, M. Modéer, P.-E. Petersson, *Analysis of crack formation and crack growth in concrete by means of fracture mechanics and finite elements*, Cement and Concrete Research,Vol 6(6), 1976, pp. 773-781.
[5] R. Huiskes , E.Y.S. Chao, *A survey of finite element analysis in orthopedic biomechanics: The first decade*, Journal of Biomechanics, Vol 16(6) 1983, pp. 385-409.
[6] O.C. Zienkiewicz, D.R.J. Owen, D.V. Phillips, G.C. Nayak , Finite element methods in the analysis of reactor vessels, Nuclear Engineering and Design, 20(2) 1972, pp. 507–541.
[7] R.H. Gallagher, Finite element analysis in brittle material design, Journal of the Franklin Institute, 290(6) 1970, pp. 523–537.
[8] R.E. Miller Jr., B.F. Backman, H.B. Hansteen, C.M. Lewis, R.A. Samuel, S.R. Varanasi, Recent advances in computerized aerospace structural analysis and design Computers & Structures, 7(2) 1977, pp. 315–326.
[9] M.Ortiz, Y.Leroy, A.Needleman, *A finite element method for localized failure analysis, Computer Methods in Applied Mechanics and Engineering*, Vol 61(2) 1987, pp. 189-214.
[10] J. Mackerle, *Finite-element analysis and simulation of machining: a bibliography (1976–1996)*, Journal of Materials Processing Technology, Vol 86, Issues 1-3, 1998, pp. 17-44.
[11] K.B. Broberg, *The foundations of fracture mechanics*, Engineering Fracture Mechanics,Vol16(4) 1982, pp. 497-515.
[12] Borst, R. De; Sluys, L.J. Muhlhaus, H.-B. Pamin, J. *Fundamental Issues In Finite Element Analyses Of Localization Of Deformation Engineering Computations*, Int J for Computer-Aided Engineering, Vol 10(2), 1993 , pp. 99-121(23).
[13] Griffith: Phil Trans Roy Soc 1921, v221, pp. 163-198.
[14] Y.Prawoto, *Quantitative failure analysis using a simple finite element approach*. Journal of Failure Analysis and Prevention, 10 (1) 2010. pp. 8-10.
[15] http://en.wikipedia.org/wiki/Nastran
[16] http://www.odonnellconsulting.com/forensicfea.html
[17] D. Momcilovic, Z. Odanovic, R.Mitrovic, I.Atanasovska, T.Vuherer, Failure analysis of hydraulic turbine shaft, Engineering Failure Analysis, 20 (2012) pp. 54–66.
[18] A.I. Karayan, A. Hersuni, D. Adisty, A. Yatim, Failure analysis of seawater inlet pipe, Journal of Failure analysis and Prevention, 11(2011) pp. 481-486.
[19] A.I. Karayan, Failure Analysis of Trunkline: An Internal Report, Center for Materials Processing and Failure Analysis (CMPFA), 2011.
[20] American Petroleum Institute (API) 5L Standard.
[21] http://octane.nmt.edu/WaterQuality/corrosion/CO2.aspx
[22] Garverick L, Corrosion in the petrochemical industry, pp. 92, ASM International, 1994.

[23] Sing B, Krishnathasan K. Pragmatic effects of flow on corrosion prediction, NACE corrosion confeence and expo 2009, Paper No. 09275.